REPORT 1136

ESTIMATION OF THE MAXIMUM ANGLE OF SIDESLIP FOR DETERMINATION OF VERTICAL-TAIL LOADS IN ROLLING MANEUVERS [1]

By RALPH W. STONE, Jr.

SUMMARY

Recent experiences have indicated that angles of sideslip in rolling maneuvers may be critical in the design of vertical tails for current research airplanes having weight distributed mainly along the fuselage. Previous investigations have indicated the seriousness of the problem for the World War II type of airplane. Some preliminary calculations for airplanes of current design, particularly with weight distributed primarily along the fuselage, are made herein.

The results of this study indicate that existing simplified expressions for calculating maximum sideslip angles to determine the vertical-tail loads in rolling maneuvers are not generally applicable to airplanes of current design. A general solution of the three linearized lateral equations of motion, including product-of-inertia terms, will usually indicate with sufficient accuracy the sideslip angles expected in aileron rolls from trimmed flight. In rolling pullouts, however, where the pitching velocity is large, consideration of cross-couple inertia terms in the equations of motion is necessary to obtain the sideslip angles accurately. The inclusion of the equation of the pitching motion seems desirable along with the lateral equations of motion in order to obtain the influence of pitching in the cross-couple inertia terms of the lateral equations. Pitching oscillations started during rolling maneuvers will be influenced by cross-couple inertia moments in pitch and may cause large variations in angle of attack which affect the horizontal-tail loads.

INTRODUCTION

Large angles of sideslip and resultant large vertical-tail loads have been encountered in a flight of a high-speed swept-wing research airplane and with models of two designs flown by the Langley Pilotless Aircraft Research Division. All three configurations rolled abruptly while pitching up. In the flight of one model, the vertical tail, which was designed by conventional methods, was lost during the rolling maneuver. The motion for all flights appeared to be essentially a rolling about the X body axis while at high angles of attack. The airplane and both models were representative of airplane configurations with weight distributed mainly along the fuselage such that the moments of inertia in pitch and yaw were much larger than the moment of inertia in roll. Thus, with regard to inertia, the airplane and models were much more prone to rolling than to yawing or pitching. The maneuvers mentioned were apparently uncontrolled and were possibly the result of the stall of one wing before the other, but the rates of roll were not abnormally high. From general considerations the existing techniques for determining critical design vertical-tail loads seem to be somewhat inadequate for some current airplane designs and mass distributions.

The problem of determining critical vertical-tail loads in rolling maneuvers had been recognized for conventional airplanes of the past decade (refs. 1 to 3). These investigations indicated that vertical-tail loads can be calculated with sufficient accuracy provided the sideslip angle, rudder deflection, and dynamic pressure are known. The investigations also presented simplified expressions for estimating the maximum sideslip angle in rolling maneuvers. The results determined by the simplified expression of reference 3 were in close agreement with results found by more rigorous expressions and with flight results for airplanes of World War II type flying in that period (1946). Examination of the simplified expressions indicates that certain assumptions and limitations were made regarding the values of some aerodynamic derivatives and ranges of mass distributions considered. Subsequent studies have indicated that these assumptions generally are not applicable for current airplane designs similar to existing research airplanes.

The vertical-tail load in a sideslip is proportional to the value of the sideslip angle and, as has been assumed in the previous work, is assumed to be a criterion for vertical-tail design. The purpose of this report is to present the results of preliminary estimations of the sideslip angle in rolling maneuvers for which the assumptions and limitations used in the simplified expressions of previous work are not included. Some preliminary estimations are also included to determine whether limitation of the motion in a rolling maneuver to the three lateral degrees of freedom, as has previously been the practice, can seriously influence the sideslip estimations.

COEFFICIENTS AND SYMBOLS

The motions presented herein were calculated about either of two systems of axes, the stability axes and the body axes, the use of either system depending on convenience. A diagram of both systems of axes showing the positive directions of the forces and moments is presented in figure 1. The coefficients and symbols presented may be considered to apply to either system of axes except where noted. Aerodynamic derivatives, normally available relative to stability axes, were transposed by the methods of reference 4 when body axes were used.

C_L lift coefficient, $\dfrac{L}{\frac{1}{2}\rho V^2 S}$

C_Y lateral-force coefficient, $\dfrac{Y}{\frac{1}{2}\rho V^2 S}$

C_l rolling-moment coefficient, $\dfrac{L'}{\frac{1}{2}\rho V^2 S b}$

C_m pitching-moment coefficient, $\dfrac{M}{\frac{1}{2}\rho V^2 S \bar{c}}$

C_n yawing-moment coefficient, $\dfrac{N}{\frac{1}{2}\rho V^2 S b}$

ΔC_l increment of rolling-moment coefficient caused by aileron deflection

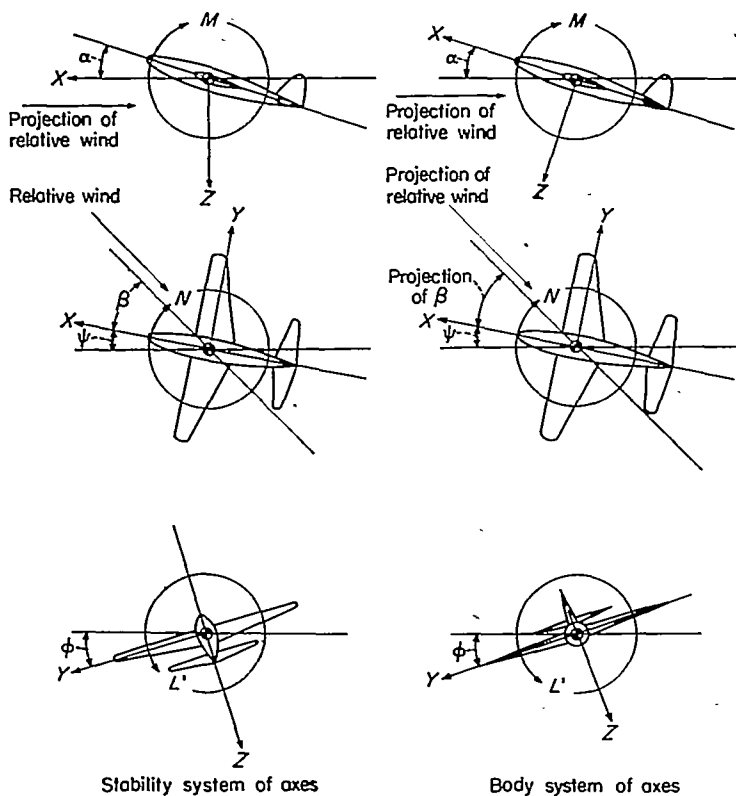ΔC_n increment of yawing-moment coefficient caused by aileron deflection

Stability system of axes   Body system of axes

FIGURE 1.—Sketch depicting the stability and body systems of axes. Each view presents a plane of the axes system as viewed along the third axis.

L	lift, lb
Y	lateral force, lb
L'	rolling moment, ft-lb
M	pitching moment, ft-lb
N	yawing moment, ft-lb
S	wing area, sq ft
b	wing span, ft
$\bar{c}$	mean aerodynamic chord, ft
ρ	air density, slugs/cu ft
V	velocity, fps
$I_{X_0}, I_{Y_0}, I_{Z_0}$	moments of inertia about X, Y, and Z principal axes, respectively, slug-ft²
I_X, I_Y, I_Z	moments of inertia about X, Y, and Z stability axes, respectively, slug-ft²
I_{XZ}	product of inertia (negative when principal axis is inclined above the flight path), slug-ft²
μ_b	relative density coefficient based on span, $m/\rho S b$
m	mass of airplane, W/g, slugs
W	weight of airplane, lb
W_Y	component of weight along Y-axis
g	acceleration due to gravity, 32.2 ft/sec²
n	normal acceleration divided by acceleration due to gravity
α	angle of attack (assumed to be equal to $\tan^{-1}\left(\dfrac{w}{u}\right)$ in the body system of axes), radians except when otherwise noted
$\Delta\alpha$	increment of angle of attack from trimmed condition
β	angle of sideslip, $\sin^{-1}\dfrac{v}{V}$, radians except when otherwise noted
u, v, w	components of velocity V along the X, Y, and Z body axes, respectively; v is also component of V along Y stability axis, fps
$\dot{v}$	rate of change of v with time
θ	angle of pitch, radians except when otherwise noted
ψ	angle of yaw, radians except when otherwise noted
ϕ	angle of roll, radians except when otherwise noted
$\dot{\phi}$ or p	rolling angular velocity, radians per second except when otherwise noted
$\dot{\theta}$ or q	pitching angular velocity, radians per second except when otherwise noted
$\dot{\psi}$ or r	yawing angular velocity, radians per second except when otherwise noted
$\dot{\beta}$	rate of change of angle of sideslip with time
$\ddot{\phi}$	rate of change of rolling angular velocity with time
$\ddot{\psi}$	rate of change of yawing angular velocity with time
$\ddot{\theta}$	rate of change of pitching angular velocity with time

$$C_{l_\beta}=\frac{\partial C_l}{\partial \beta}$$

$$C_{n_\beta}=\frac{\partial C_n}{\partial \beta}$$

$$C_{Y_\beta}=\frac{\partial C_Y}{\partial \beta}$$

$$C_{l_p}=\frac{\partial C_l}{\partial \frac{pb}{2V}}$$

$$C_{n_p}=\frac{\partial C_n}{\partial \frac{pb}{2V}}$$

$$C_{l_r}=\frac{\partial C_l}{\partial \frac{rb}{2V}}$$

$$C_{n_r}=\frac{\partial C_n}{\partial \frac{rb}{2V}}$$

$$C_{m_\alpha}=\frac{\partial C_m}{\partial \alpha}$$

$$C_{m_q}=\frac{\partial C_m}{\partial \frac{q\bar{c}}{2V}}$$

GENERAL CONSIDERATIONS

Consideration has been given to various existing methods for calculating angles of sideslip in rolling maneuvers. Limitations in these procedures which may critically influence the sideslip angles for airplanes of current design have been investigated and are discussed briefly herein.

Simplified expressions, as has previously been noted, are presented in previous studies for the determination of the maximum sideslip angle in rolling maneuvers. The simplified expression of reference 1 gives the sideslip angle necessary to balance combined yawing moments caused by the ailerons (ΔC_n) and by rolling (C_{n_p}). The expression of reference 3 is the same as that of reference 1 but with an analytic empirical factor of 2 and is

$$\beta_{max}=\frac{1}{4}\frac{\Delta C_l}{C_{l_p}}\frac{C_L}{C_{n_\beta}} \qquad (1)$$

Stability studies subsequent to the study of reference 3, such as references 5 and 6, have indicated that the assumptions used in this simplified expression are not applicable for some current configurations. Also, the range of mass parameters used to evaluate this expression was limited; the ratio of values of I_Z/I_X studied in reference 3 was from $1\frac{1}{3}$ to $3\frac{1}{3}$, whereas some current high-speed airplane designs have ratios of the order of 5 to 12. The effect of these differences for current airplane designs should be evaluated to justify any further use of the simplified expression (eq. (1)).

A more rigorous expression used to set up design charts for the maximum sideslip angle in rolling maneuvers is also presented in reference 3. This expression is based on the linearized lateral equations of motion in which the product-of-inertia terms have been omitted. With the advent of the fuselage-heavy loadings the product-of-inertia terms will be large, particularly at high angles of attack, and may influence the motion and the maximum angle of sideslip in rolling maneuvers. An evaluation of the effects of products of inertia on the maximum sideslip angles estimated in rolling maneuvers for airplanes of current designs therefore should be made.

Another point for consideration in estimating sideslip angles in rolling maneuvers, particularly when rolls occur in pull-ups, may be cross-couple inertia moments which exist when both lateral and longitudinal motions occur together. The effects of cross-couple inertia moments may be particularly important when the weight is distributed primarily along the fuselage. It is believed therefore that the effects of these cross-couple inertia moments on the sideslip angle in rolling maneuvers also should be evaluated.

METHOD OF ANALYSIS

In order to evaluate the effects of the various parameters and changes in parameters which may influence estimates of sideslip angles in rolling maneuvers of current airplane configurations, a preliminary study of rolling maneuvers of two airplane configurations was made. Calculations were made of the variation of sideslip angle with time in rolling maneuvers by an analytic solution of the linearized lateral equations of motion, both with and without product-of-inertia terms, and by a step-by-step integration of equations of motion that are more complete than the linearized lateral equations of motion. The maximum angle of sideslip was also calculated by use of the simplified expression of reference 3 (eq. (1)).

The three linearized lateral equations of motion used, with product-of-inertia terms included, are

$$\left.\begin{aligned} I_X\ddot{\phi}-I_{XZ}\ddot{\psi}-\left(C_{l_\beta}\beta+C_{l_p}\frac{\dot{\phi}b}{2V}+C_{l_r}\frac{\dot{\psi}b}{2V}+\Delta C_l\right)\frac{1}{2}\rho V^2 Sb=0 \\ I_Z\ddot{\psi}-I_{XZ}\ddot{\phi}-\left(C_{n_\beta}\beta+C_{n_p}\frac{\dot{\phi}b}{2V}+C_{n_r}\frac{\dot{\psi}b}{2V}+\Delta C_n\right)\frac{1}{2}\rho V^2 Sb=0 \\ mV(\dot{\beta}+\dot{\psi})-\left(\frac{C_L}{n}\phi+C_{Y_\beta}\beta\right)\frac{1}{2}\rho V^2 S=0 \end{aligned}\right\} \quad (2)$$

Solution of these equations was made relative to the stability system of axes.

In order to evaluate the effects of cross-couple inertia terms on rolling and yawing motions, the pitching velocity must be included; therefore a fourth degree of freedom is necessary, the pitching degree of freedom. It was assumed that changes in accelerations along the X- and Z-axes would not be sufficient in the time necessary to roll 90° to influence the resultant motion greatly. Because the cross-couple inertia terms are nonlinear, an analytic solution was not

possible and a step-by-step integration was made. The step-by-step method used was Euler's method, briefly outlined in reference 7. Euler's dynamical equations for the four degrees of freedom are

$$
\left.
\begin{aligned}
L' &= I_{x_0}\ddot{\phi} - (I_{y_0} - I_{z_0})\dot{\theta}\dot{\psi} \\
M &= I_{y_0}\ddot{\theta} - (I_{z_0} - I_{x_0})\dot{\phi}\dot{\psi} \\
N &= I_{z_0}\ddot{\psi} - (I_{x_0} - I_{y_0})\dot{\phi}\dot{\theta} \\
Y &= m(\dot{v} + u\dot{\psi} - w\dot{\phi}) - W_Y
\end{aligned}
\right\}
\qquad (3)
$$

Solution of these equations was made relative to the body axes (assumed to be the principal axes); therefore product-of-inertia terms do not appear. These equations as used in the step-by-step integration were written as follows:

$$
I_{x_0}\ddot{\phi} - (I_{y_0} - I_{z_0})\dot{\theta}\dot{\psi} -
$$
$$
\left(C_{l_\beta}\beta + C_{l_p}\frac{\dot{\phi}b}{2V} + C_{l_r}\frac{\dot{\psi}b}{2V} + \Delta C_l\right)\frac{1}{2}\rho V^2 S b = 0 \quad (4a)
$$

$$
I_{y_0}\ddot{\theta} - (I_{z_0} - I_{x_0})\dot{\phi}\dot{\psi} - \left(C_{m_\alpha}\Delta\alpha + C_{m_q}\frac{\dot{\theta}\bar{c}}{2V}\right)\frac{1}{2}\rho V^2 S \bar{c} = 0 \quad (4b)
$$

$$
I_{z_0}\ddot{\psi} - (I_{x_0} - I_{y_0})\dot{\phi}\dot{\theta} -
$$
$$
\left(C_{n_\beta}\beta + C_{n_p}\frac{\dot{\phi}b}{2V} + C_{n_r}\frac{\dot{\psi}b}{2V} + \Delta C_n\right)\frac{1}{2}\rho V^2 S b = 0 \quad (4c)
$$

$$
mV(\cos\beta\dot{\beta} + \dot{\psi}\cos\alpha - \dot{\phi}\sin\alpha) - W\sin(\phi\cos\alpha + \psi\sin\alpha) -
$$
$$
C_{Y_\beta}\beta\frac{1}{2}\rho V^2 S = 0 \quad (4d)
$$

The expression for the weight component in the side-force equation (4d) is approximate but is considered to be sufficiently accurate provided the angle of attack does not become excessively large or have large variations.

In order to evaluate the angle of attack for use in equations (4), an additional equation was used whereby the angle of attack was estimated for each step of the calculations.

For all calculations made the maneuver was considered to be initiated by an abrupt aileron deflection, the rudder being held fixed. The aileron deflection was considered to be constant throughout the maneuver. The motion was presumed to take place approximately in a horizontal plane for all calculations. These assumptions are conservative in that they result in somewhat larger estimated sideslip angles than those that would be obtained in actual flight where a finite time is required to reach maximum aileron deflections or where the motion is not in a horizontal plane, as may be true particularly for a roll in a pull-up. For the case of the pull-up maneuver the assumption was made that the initial pitching velocity had no influence on changes in the angle of attack but that only additional pitching velocities affected this angle.

CALCULATIONS

The sideslip angles were calculated by each of the various methods for two airplanes having different stability derivatives. The aerodynamic and physical parameters for the two airplanes are listed in table I. The aerodynamic parameters and stability derivatives for airplane A (table I) are

those which might be representative of an airplane having a long fuselage and a short-span thin wing. It should be noted that the stability derivatives C_{n_β} and C_{l_β} are relatively large. The aerodynamic characteristics for airplane B (table I) were taken from configuration 1 of reference 3; the necessary pitching derivatives were assumed. For this case the values of C_{n_β} and C_{l_β} were considerably smaller than those of airplane A. In order to make computations of sideslip for a condition similar to one for configuration 1 of reference 3, the value of ΔC_l of airplane B was taken to make $\dfrac{\Delta C_l}{C_{l_p}}\dfrac{C_L}{C_{n_\beta}}$ equal to 120 and the value of ΔC_n was taken as equal to $\dfrac{\Delta C_l}{C_{l_p}}\dfrac{C_L}{16}$. The value of C_{n_p} used for these calculations was assumed to be constant throughout the rolling motion. The effect of aileron deflection on the rotary wash of the wing at the tail was not included in the value of C_{n_p} used. For specific cases, however, consideration of this effect should be made. In addition, because the motions considered herein have accelerations in roll, a lag in the rotary wash of the wing at the tail will exist and will affect the value of the moment $C_{n_p}\dfrac{pb}{2V}$ acting at any given instant. Consideration of this effect should be made in a specific case. A discussion of the rotary wash of the wing on the tail is given in reference 6.

The mass characteristics used for the calculations on each of the two airplanes are listed in table II. Two loadings

TABLE I.—AERODYNAMIC AND DIMENSIONAL CHARACTERISTICS

[Aerodynamic characteristics are referred to stability axes]

	Airplane A	Airplane B
Wing area, sq ft	166. 5	248
Wing span, ft	22. 7	38. 3
Mean aerodynamic chord, ft	7. 84	6. 87
C_{l_β}, per degree	−0. 0032	−0. 0010
C_{n_β}, per degree	0. 0065	0. 00040
C_{Y_β}, per degree	−0. 015	−0. 0075
C_{l_p}, per radian	−0. 225	−0. 455
C_{n_p}, per radian	−0. 130	−0. 044
C_{l_r}, per radian	0. 235	0. 198
C_{n_r}, per radian	−1. 090	−0. 0069
C_{m_q}, per radian	−9. 000	−9. 000
C_{m_α}, per degree	−0. 0167	−0. 0174
ΔC_l	0. 0197	0. 0242
ΔC_n	−0. 0035	−0. 00209

TABLE II.—MASS CHARACTERISTICS

Loading	Weight, lb	Airplane relative density coefficient, μ_1	Moments of inertia, slug-ft²		
			I_{x_0}	I_{y_0}	I_{z_0}
Airplane A					
1	20, 828	71. 9	5, 381	63, 971	65, 550
2	20, 828	71. 9	34, 676	63, 676	65, 550
Airplane B					
1	21, 800	30	14, 900	20, 000	39, 750
2	21, 800	30	5, 381	63, 971	65, 559

were used for each airplane. For airplane A loading 1 was such that $I_z \approx 12 I_x$ and $I_Y - I_x \approx 11 I_x$ and loading 2 was such that $I_z \approx 2 I_x$ and $I_x - I_Y = 0$. Loading 1 for airplane B was taken for configuration 1 of reference 3 for $\mu_b = 30$; a pitching moment of inertia was assumed. Loading 2 for airplane B was similar to loading 1 of airplane A.

Estimations of the sideslip angles in rolling maneuvers were made for each of the various methods for the flight conditions of table III.

The calculations were based on sea-level air density ρ of 0.002378. The motion for each flight condition was calculated by each of the various methods through approximately 90° of roll. For the step-by-step solutions the aerodynamic derivatives, referred to the body axes, were assumed to be constant and thus independent of angle of attack for the range of angle of attack obtained. For the analytic solution of the lateral equations of motion the angle of attack is assumed to be constant and thus, of course, the aerodynamic derivatives are also constant.

The results for the step-by-step solutions are presented in figures 2 to 6 for the various conditions listed in table III. Shown in figures 2 to 6 are the variations of angular displacement and angular velocity about the three body axes with time, as well as the variation of the angle of sideslip and the angle of attack with time. The results for the analytic solutions of the three lateral equations of motion both with and without the effects of products of inertia of the variation of the sideslip angle with time for the various conditions listed in table III are presented in figures 7 to 11. The variation of sideslip angle with time for the step-by-step solutions is also presented in figures 7 to 11 for comparative purposes.

In the step-by-step procedure, an increment of time is used which in general should be relatively small. A sufficiently small increment of time should be chosen so as to obtain the proper result. In general, large time increments tend to indicate a less stable motion and thus may indicate larger maximum values of sideslip than may actually exist. If the motions tend to be irregular, smaller increments of time may be necessary than when the variations of the motion are small. As an example of the effect of different time increments, the trimmed flight solution for airplane A, loading 1, was briefly studied for three time increments; the effects on the sideslip angle are shown in figure 12. For the step-by-step calculations presented herein, brief studies were made of the effects of time increments and sufficiently small values were used so that the maximum sideslip angle may be considered to be accurate within $\frac{1°}{2}$.

TABLE III.—FLIGHT CONDITIONS FOR CALCULATIONS

| Airplane	Loading	Flight condition	Initial angle of attack, deg	C_L	V, fps
A	1	Aileron roll from trimmed flight	10	0.6	419
A	2	Aileron roll from trimmed flight	10	.6	419
A	1	6g pullout	13	.78	900
B	1	Aileron roll from trimmed flight	12	.9	286
B	2	Aileron roll from trimmed flight	12	.9	286
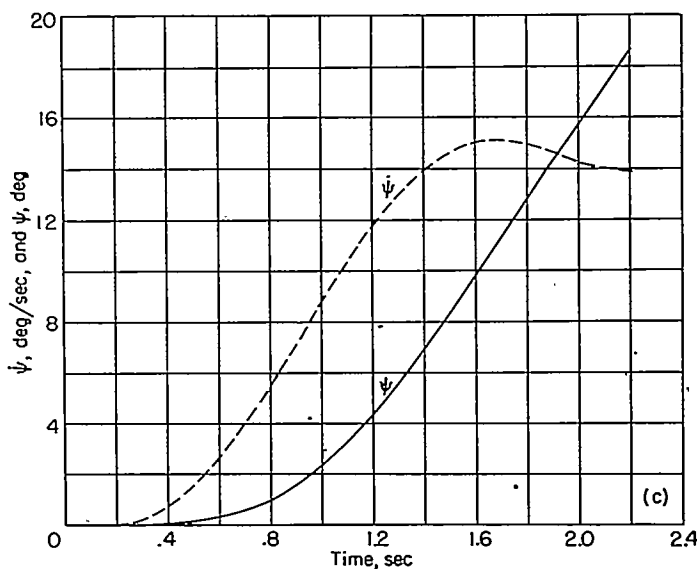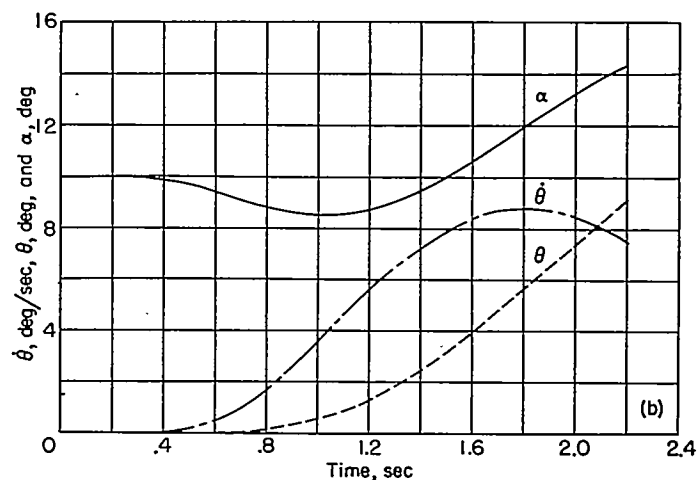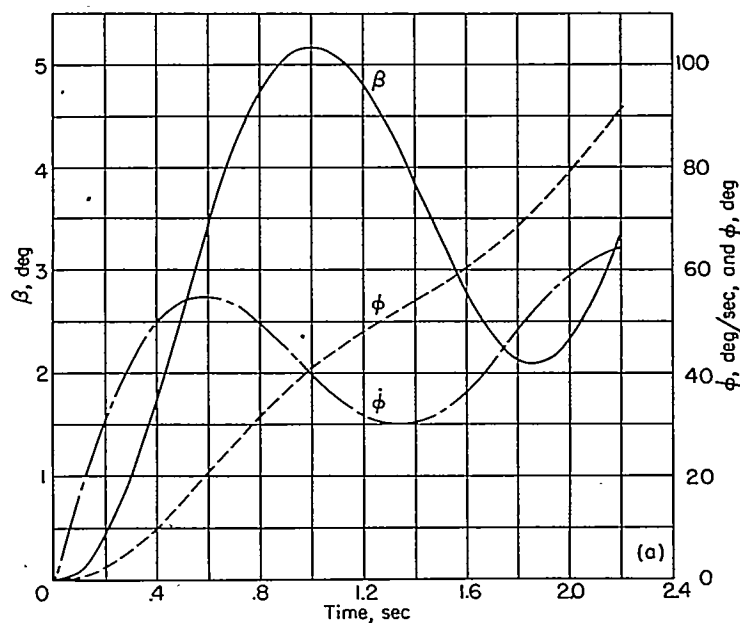
(a) β, ϕ, and $\dot{\phi}$.
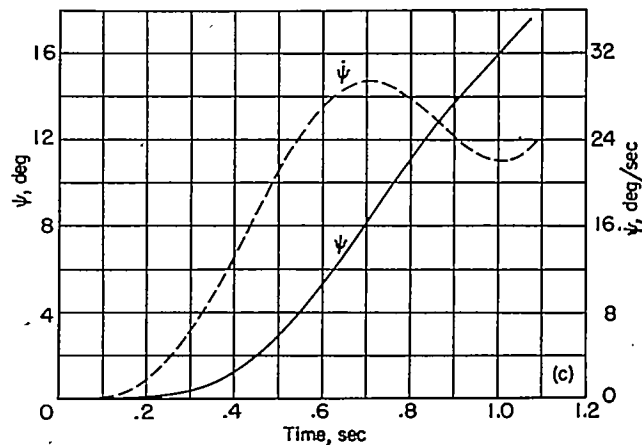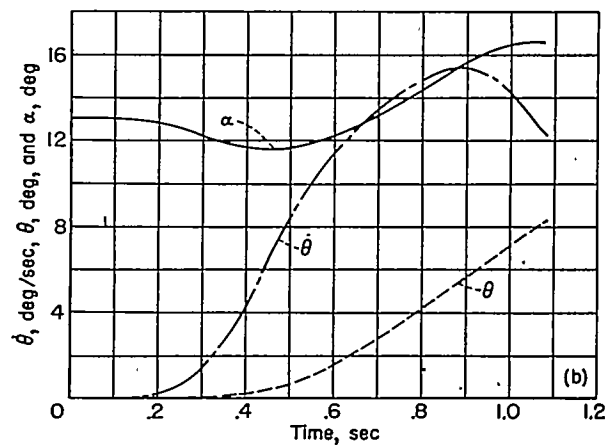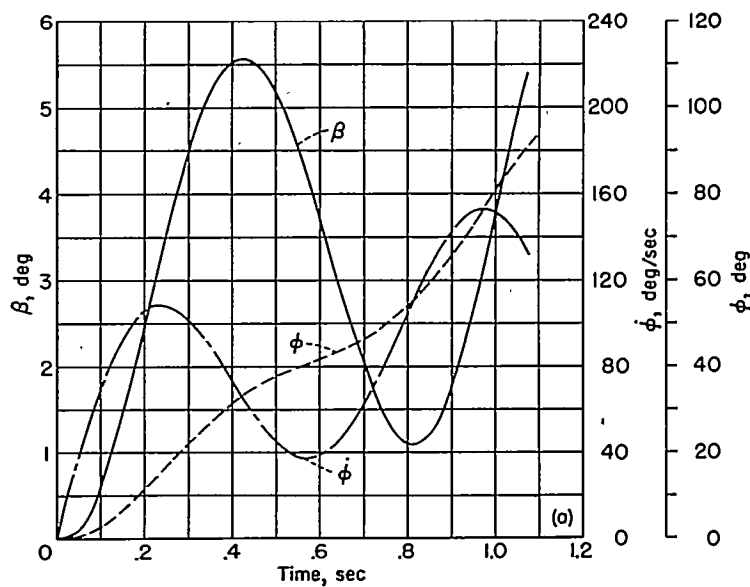(b) α, θ, and $\dot{\theta}$.
(c) ψ and $\dot{\psi}$.

FIGURE 2.—Motion of airplane A, heavily loaded along the fuselage (loading 1), when rolled from trimmed flight at an angle of attack of 10°. Step-by-step method.

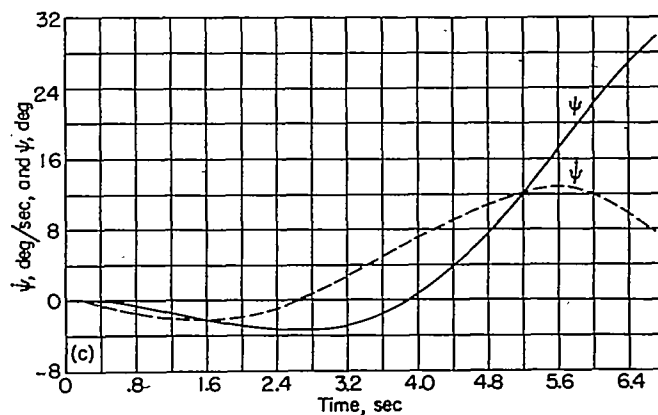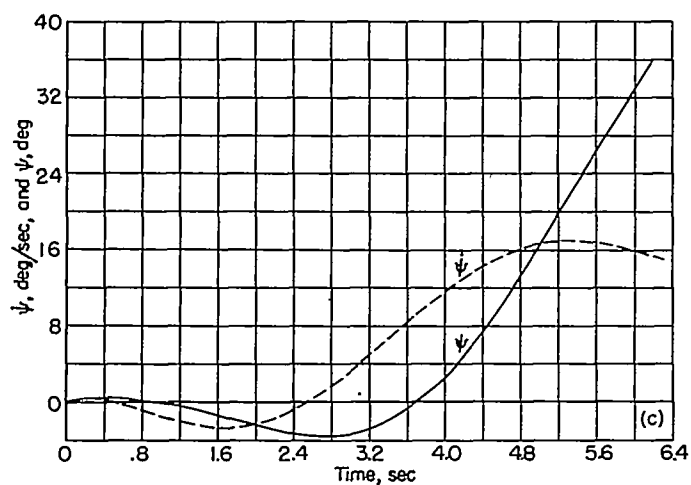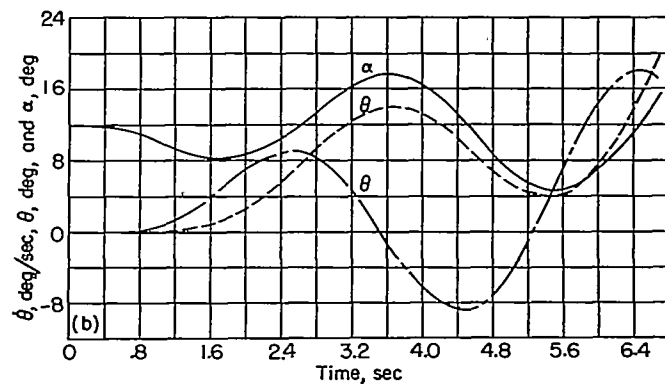(a) β, ϕ, and $\dot\phi$.

(b) α, θ, and $\dot\theta$.
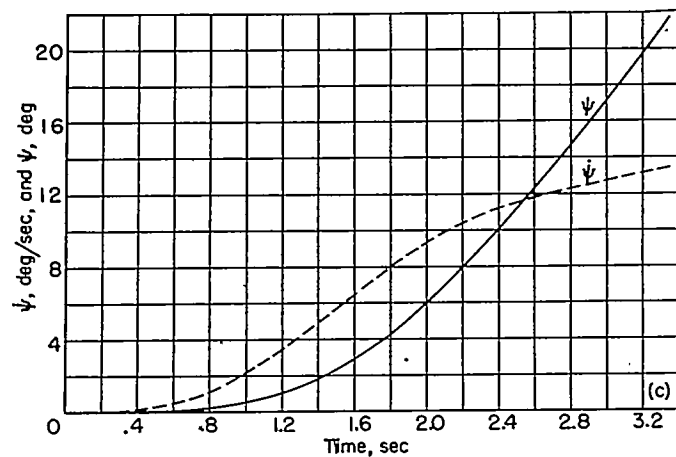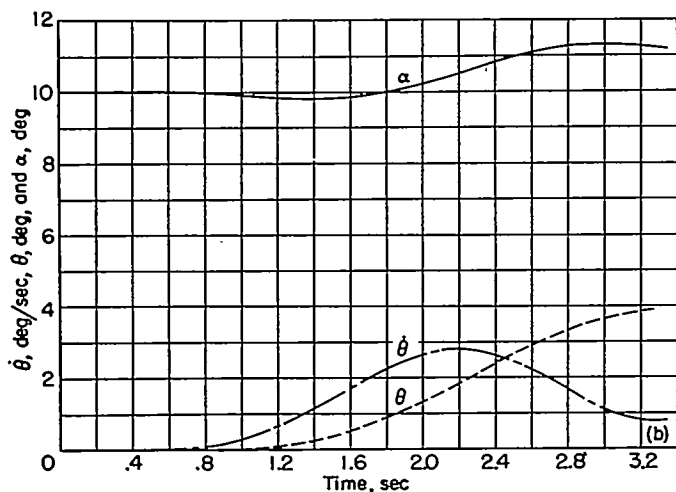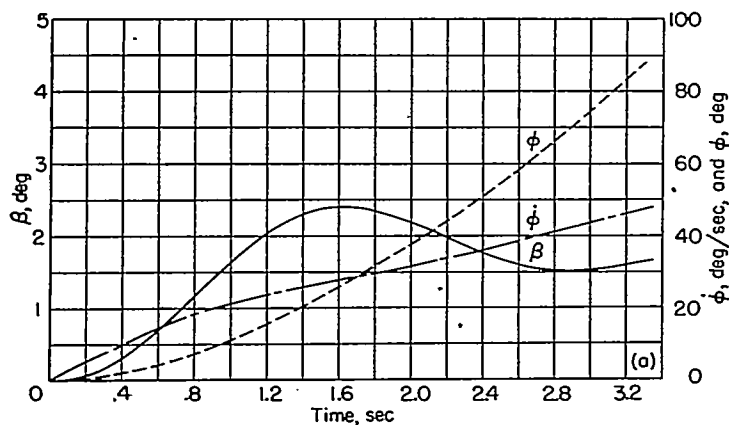
(c) ψ and $\dot\psi$.

FIGURE 3.—Motion of airplane A, equally loaded along the wings and the fuselage (loading 2), when rolled from trimmed flight at an angle of attack of 10°.   Step-by-step method.

(a) β, ϕ, and $\dot\phi$.

(b) α, θ, and $\dot\theta$, where θ is an increment added to the initial pitching velocity.

(c) ψ and $\dot\psi$.

FIGURE 4.—Motion of airplane A, heavily loaded along the fuselage (loading 1), when rolled in a 6g pull-out.   Step-by-step method.
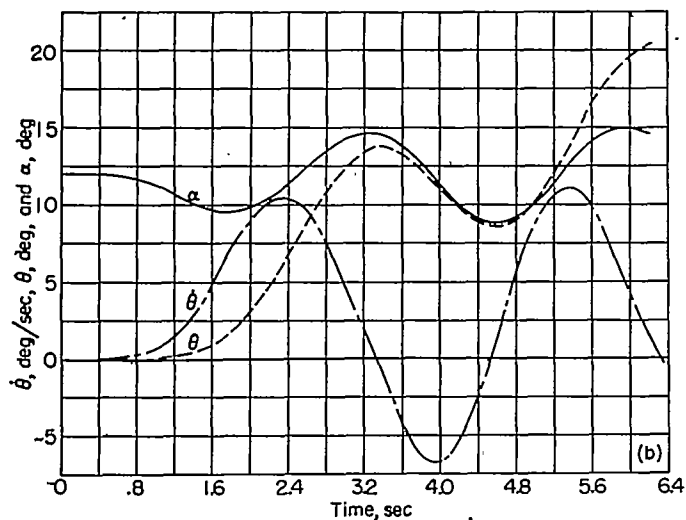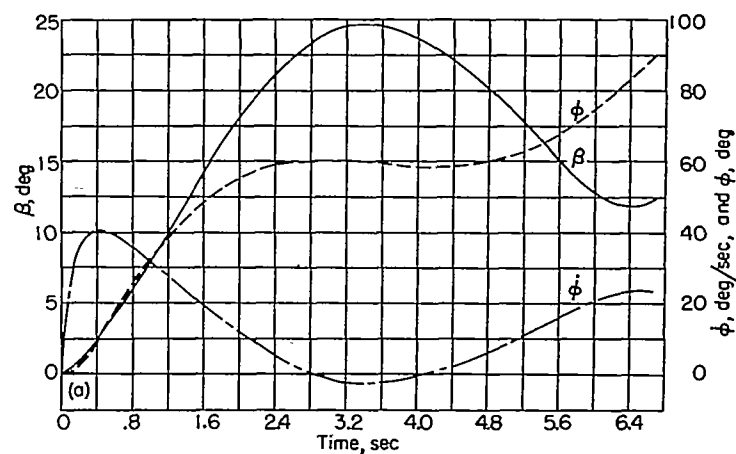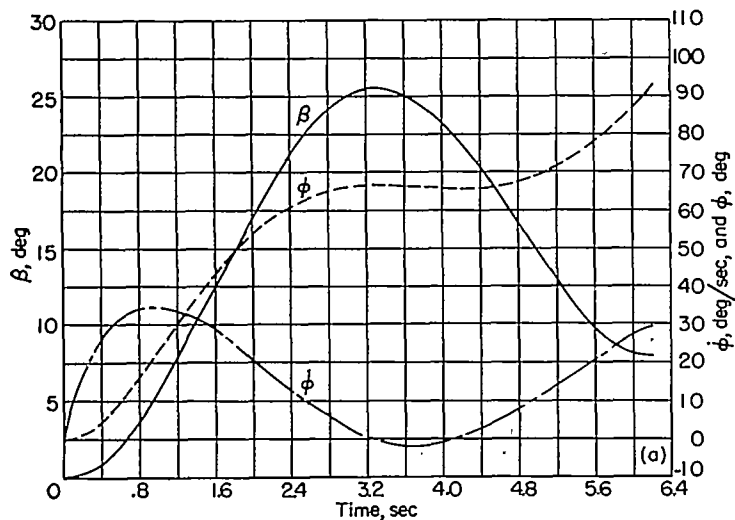
(a) β, ϕ, and $\dot{\phi}$.
(b) α, θ, and $\dot{\theta}$.
(c) ψ and $\dot{\psi}$.

FIGURE 5.—Motion of airplane B, normal mass distribution (loading 1), when rolled from trimmed flight at an angle of attack of 12°. Step-by-step method.

(a) β, ϕ, and $\dot{\phi}$.
(b) α, θ, and $\dot{\theta}$.
(c) ψ and $\dot{\psi}$.

FIGURE 6.—Motion of airplane B, heavily loaded along the fuselage (loading 2), when rolled from trimmed flight at an angle of attack of 12°. Step-by-step method.

RESULTS AND DISCUSSION

AIRPLANE A

The results for airplane A with the mass distributed mostly along the fuselage (loading 1) show that by the step-by-step method a maximum sideslip of about $5\frac{1}{4}°$ was obtained (fig. 2). The solution of the linearized lateral equations of motion, including product-of-inertia terms, gave a maximum sideslip angle of about $4\frac{3}{4}°$; whereas the solution of the linearized lateral equations without product-of-inertia terms gave a maximum sideslip angle of $4\frac{1}{2}°$ (fig. 7). Solution of the simplified expression of reference 3 (eq. (1)) gives a result for the maximum sideslip angle of only 2°.

The results for airplane A for the second loading where I_X and I_Y were equal and each approximately one-half of I_Z show a maximum angle of sideslip of about $2\frac{1}{2}°$ by the step-by-step calculations (fig. 3). The solution of the linearized lateral equation of motion, including product-of-inertia terms, gave a maximum angle of sideslip of about $2\frac{1}{4}°$ and the solution without product-of-inertia terms gave

a maximum sideslip angle of approximately 2° (fig. 8). The simplified expression of reference 3, equation (1), gives a value of maximum sideslip angle of 2°.

The results for the 6g pull-up for airplane A, loading 1, (fig. 4) are for a relatively high velocity of 900 feet per second (Mach number of approximately 0.83). (The stability derivatives in table I for airplane A were used without consideration of any compressibility effects.) A maximum angle of sideslip of approximately $5\frac{1}{2}°$ was obtained by the step-by-step method. The linearized lateral equations of motion, including product-of-inertia terms, gave a maximum angle of sideslip of about $4\frac{1}{2}°$ (fig. 9); whereas the linearized lateral equations excluding product-of-inertia terms gave a maximum sideslip angle of only $2\frac{1}{2}°$. The simplified expression of reference 3 (eq. (1)) gives a maximum
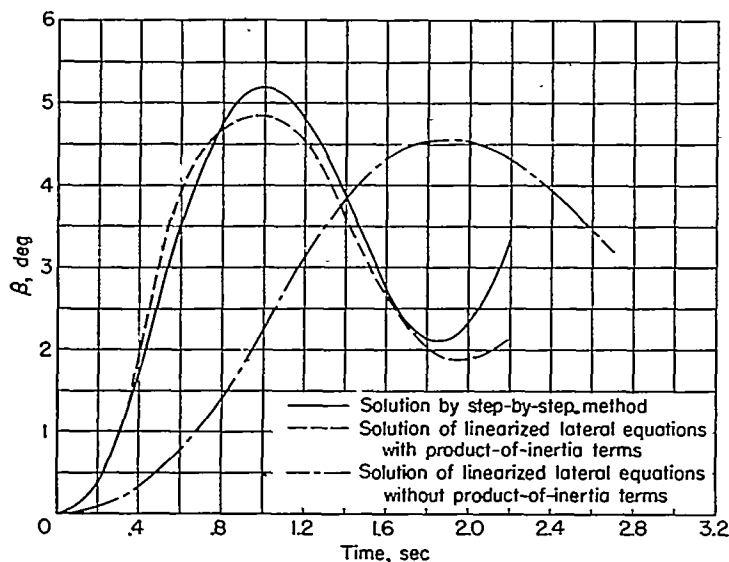

FIGURE 7.—Comparison of a solution by step-by-step method and a solution of linearized lateral equations of the variation of angle of sideslip with time for airplane A, loading 1, when rolled from trimmed flight at an angle of attack of 10°.
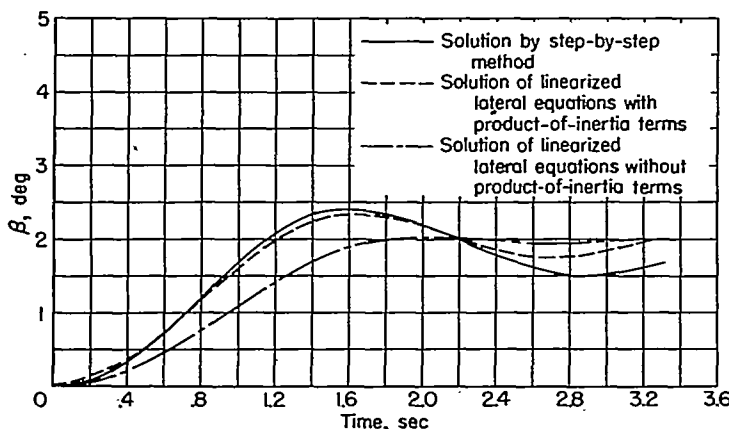

FIGURE 8.—Comparison of a solution by step-by-step method and a solution of linearized lateral equations of the variation of angle of sideslip with time for airplane A, loading 2, when rolled from trimmed flight at an angle of attack of 10°.

FIGURE 9.—Comparison of a solution by step-by-step method and a solution of linearized lateral equations of the variation of angle of sideslip with time for airplane A, loading 1, when rolled in a 0g pullout.
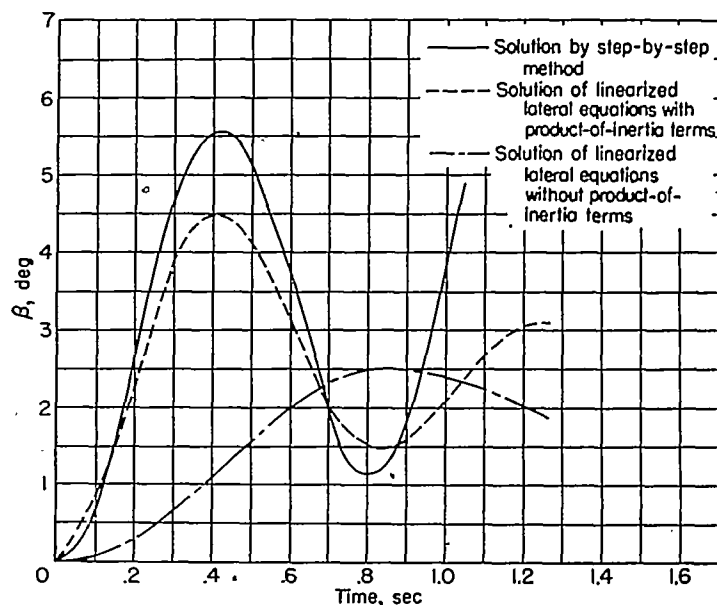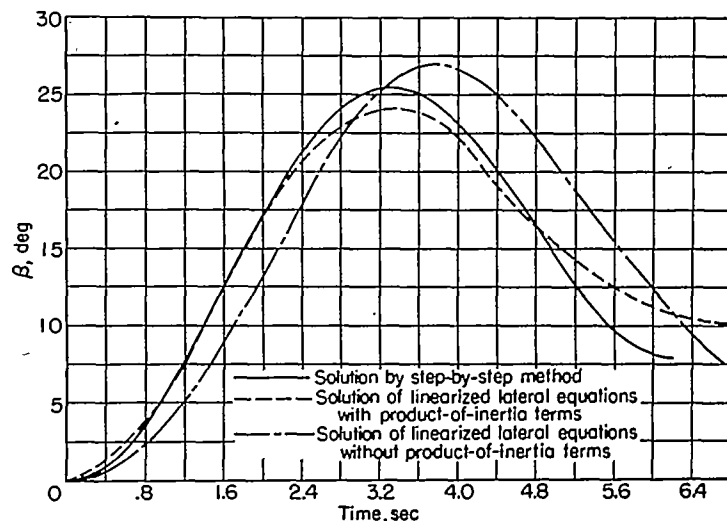

FIGURE 10.—Comparison of a solution by step-by-step method and a solution of linearized lateral equations of the variation of angle of sideslip with time for airplane B, loading 1, when rolled from trimmed flight at an angle of attack of 12°.

value of sideslip angle for this case of about $2\frac{1}{2}°$. It may be of interest to note that the value of maximum sideslip angle obtained for the rolling pull-up by the more complete methods was somewhat in excess of the maximum values for which similar recent research airplanes have been designed.

A summarization of these results for the maximum angles of sideslip for each airplane condition and method of calculation is presented in table IV. The values listed are approximate in that they have been rounded to the nearest $\frac{1}{4}°$.

The results of airplane A for aileron rolls in trimmed flight (loadings 1 and 2) by the step-by-step method and by a solution of the linearized lateral equations, including product-of-inertia terms, compare favorably both in the maximum sideslip and its variation with time (figs. 7 and 8). It appears, therefore, that the pitching velocities which are included in the step-by-step solutions did not appreciably influence the sideslip angles through the cross-couple inertia moments in yaw $(I_X-I_Y)\dot\theta\dot\phi$ and roll $(I_Y-I_Z)\dot\theta\dot\psi$. The solution of the linearized lateral equations of motion, including product-of-inertia terms, therefore appears to be adequate for estimating the maximum angle of sideslip when the pitching motion is relatively small.

For the case of the $6g$ pull-up, however, the linearized solution underestimated the maximum sideslip angle obtained by the step-by-step solution by approximately 20 percent and the variation of sideslip angle with time (fig. 9) is somewhat different for the solution of the linearized lateral equations (including product-of-inertia terms) and for the step-by-step solution. The periods of the motion for the two solutions are similar but the damping characteristics appear to be considerably different. This difference is in agreement with reference 8 which indicates that in steady rolling cross-couple inertia moments cause changes in stability when the directional and longitudinal stabilities are different. The differences indicate some influence of the

pitching motion on the lateral motion through the cross-couple inertia moments resulting from the pitching, these moments being $(I_X-I_Y)\dot\phi\dot\theta$ and $(I_Y-I_Z)\dot\psi\dot\theta$ for yawing and rolling, respectively. This effect for the pull-up case appears to be the result of the much larger pitching velocity associated with the pullout maneuver than existed for the aileron rolls from trimmed flight where the agreement by the two solutions was good both for the maximum sideslip as well as its variation with time (figs. 7 and 8). It appears therefore that, for rolls in pullouts when the pitching velocity is large, sideslip angles should be calculated by the more complete step-by-step method of the nonlinear equations of motion which include cross-couple inertia terms.
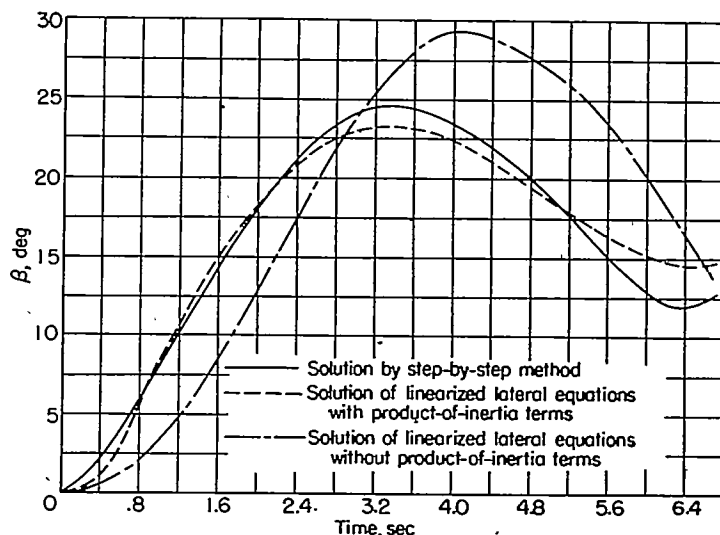

FIGURE 11.—Comparison of a solution by step-by-step method and a solution of linearized lateral equations of the variation of angle of sideslip with time for airplane B, loading 2, when rolled from trimmed flight at an angle of attack of 12°.
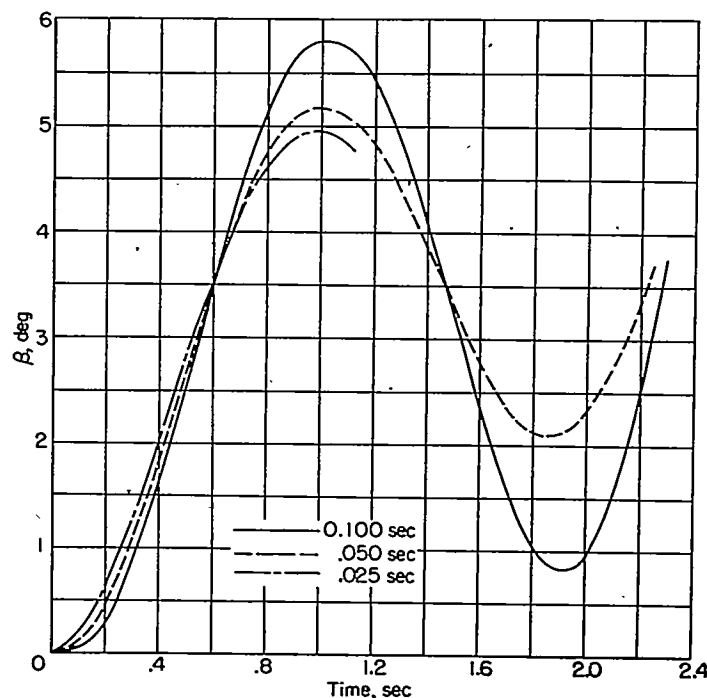
FIGURE 12.—Effects of different time increments on the variation with time and the maximum value of sideslip angle for airplane A, loading 1, when rolling from trimmed flight at an angle of attack of 10°. Step-by-step method.

TABLE IV.—SUMMARY OF MAXIMUM SIDESLIP ANGLES OBTAINED IN ROLLING MANEUVERS FOR THE VARIOUS CONDITIONS CONSIDERED AND BY THE VARIOUS METHODS USED

Loading	Flight condition	Sideslip angle, deg, obtained by—			
		Step-by-step solution	Solution of linearized lateral equations with product-of-inertia terms	Solution of linearized lateral equations without product-of-inertia terms	Solution of simplified expression (eq. (1))
Airplane A					
1	Aileron roll from trimmed level flight	$5\frac{1}{4}$	$4\frac{3}{4}$	$4\frac{1}{2}$	2
2	Aileron roll from trimmed level flight	$2\frac{1}{4}$	$2\frac{1}{4}$	2	2
1	Roll from $6g$ pullout	$5\frac{1}{2}$	$4\frac{1}{2}$	$2\frac{1}{4}$	$2\frac{1}{4}$
Airplane B					
1	Aileron roll from trimmed level flight	$25\frac{1}{4}$	24	27	30
2	Aileron roll from trimmed level flight	$24\frac{1}{2}$	$23\frac{1}{4}$	30	30

The rate of roll $\dot{\phi}$ for airplane A, loading 1, both for the aileron roll from trimmed flight and the 6g pullout (figs. 2 and 4) varied considerably during part of the motion, apparently being dependent upon the sideslip angle and upon C_{l_β} (the dihedral effect). A maximum value of $pb/2V$ of about 0.03 was obtained for both cases; whereas the value of $\Delta C_l/C_{l_p}$, the steady-state value of $pb/2V$ for the rolling degree of freedom, would be about 0.088 for both cases. For loading 2 (where the weight is more heavily distributed along the wing than for loading 1) the airplane rolled slower than for the first loading and the maximum value of $pb/2V$ attained was about 0.023 as compared again with the value of $\Delta C_l/C_{l_p}$ of 0.088. Since the simplified expression of reference 3 (eq. (1)) is based on a substitution of $\Delta C_l/C_{l_p}$ for $pb/2V$, agreement in these parameters appears essential to the valid use of equation (1). For airplane A these parameters were appreciably different. For loading 1 either for the aileron roll from trimmed flight or the 6g pullout, the simplified expression appreciably underestimated the value of maximum sideslip angle. Because of differences in the values of $\Delta C_l/C_{l_p}$ and $pb/2V$ the agreement indicated by the simplified expression and other methods of calculation for airplane A, loading 2 (aileron roll from trimmed flight), appears to be only coincidental. It appears, therefore, that the simplified expression is not generally applicable for airplanes of the type of airplane A.

The effects of products of inertia on the maximum angle of sideslip and its variation with time are shown by the comparison of the solutions of the lateral equations both with and without products of inertia in figures 7 to 9 for the various conditions calculated for airplane A. Solutions without the product-of-inertia terms underestimated the maximum sideslip angle as obtained by the more complete methods of calculation. The effect of the products of inertia on the sideslip angle appears to be primarily an effect on the yawing moment, where the component of moment is $\dot{\phi}I_{xz}$. In general this effect (for negative values of I_{xz} as exist for the cases considered herein) is to increase the maximum sideslip angle, provided $\dot{\phi}$ is positive prior to the time the maximum sideslip angle is reached. It is also of interest to note that products of inertia had an appreciable influence on the period of the motion as well as the damping of the motion for this airplane as calculated by the linearized lateral equations, both the period and time to damp of the oscillations being shortened by the products of inertia (table V).

As has previously been indicated, the pitching motion and the resulting cross-couple inertia moments do not appreciably influence the motion or the maximum sideslip angle for the aileron rolls from trimmed flight (figs. 7 and 8). The differences between the results for loadings 1 and 2 thus seem to be caused by the differences in the value of I_x, loading 2 leading to a smaller value of maximum sideslip. Because

of the increased value of I_x for the second loading, the airplane rolled slower than for the first loading; hence at a given instant of time $pb/2V$ was smaller and the moment $C_{n_p}\dfrac{pb}{2V}$ which was in a direction to increase the sideslip angle was smaller than for the first loading. Airplanes which roll fast may therefore tend to encounter larger values of maximum sideslip than those which roll slow.

As an extreme example of the effects of inertia, consider a case of infinite inertia about the Z- and Y-axes and some finite inertia about the X-axis. Rolling about the X body axis would cause maximum sideslip angles equal to the initial angle of attack, and the angle of attack would vary through a range of plus and minus the initial value of angle of attack. It is apparent, therefore, that the initial angle of attack is important to any study made and that the most serious condition would be one of the rolling pullout where the angle of attack is large and the speed is high.

As is implied in the previous discussion, when the rolling motion of an airplane is considered about the body axis, increased roll results in decreased angle of attack. Because the airplane has static stability (and a finite value of I_Y), the airplane tended to maintain its original trim angle for airplane A, and a pitching oscillation was started (figs. 2 (b), 3 (b), and 4 (b)). The cross-couple inertia moment in pitch $(I_z—I_x)\dot{\phi}\dot{\psi}$ for all cases for airplane A was in a direction to cause the airplane to trim at angle of attack greater than the original trim angle because $\dot{\phi}$ and $\dot{\psi}$ were both always positive, as is $I_z—I_x$.

AIRPLANE B

The results of step-by-step calculations for airplane B, loading 1 (configuration 1 of ref. 3), gave a value of maximum angle of sideslip of approximately $25\tfrac{1}{2}°$ (fig. 5). The solution

TABLE V.—LATERAL OSCILLATORY STABILITY FOR CONDITIONS CALCULATED

Flight condition	Loading	Product-of-inertia effects included		Product-of-inertia effects excluded	
		Period of oscillation, sec	Time to damp to one-half amplitude, sec	Period of oscillation, sec	Time to damp to one-half amplitude, sec
Airplane A					
Aileron roll from trimmed level flight	1	1.98	1.85	2.83	78.1
Aileron roll from trimmed level flight	2	2.83	3.62	2.95	3.80
Roll from 6g pullout	1	.84	.57	1.34	2.36
Airplane B					
Aileron roll from trimmed level flight	1	6.61	5.52	6.85	42.7
Aileron roll from trimmed level flight	2	8.40	2.89	7.95	22.5

of the linearized lateral equations of motion, including product-of-inertia terms, gave a maximum sideslip angle of about 24°; whereas the solution of the linearized lateral equations of motion without product-of-inertia terms gave a maximum sideslip angle of about 27° (fig. 10). The simplified expression of reference 3 (eq. (1)) gives a value of approximately 30°.

The results for the second loading for airplane B (fig. 6) indicate that a maximum sideslip angle of about $24\frac{1}{2}°$ was attained by the step-by-step method. The solution of the linearized lateral equations of motion, including product-of-inertia terms, gave a maximum sideslip angle of about $23\frac{1}{4}°$ which compares favorably with the value of $24\frac{1}{2}°$ obtained by the step-by-step method. The variation of sideslip angle with time also compares favorably for the two methods (fig. 11). A solution of the linearized lateral equations, excluding product-of-inertia effects, gave a maximum sideslip angle of about 30°. The simplified expression of reference 3 (eq. (1)) gives a maximum sideslip angle of about 30° for this case.

These results of approximate maximum sideslip angles for airplane B are listed in table IV. As was indicated for airplane A, the values in table IV have been rounded to the nearest $\frac{1}{4}°$.

As was the case for airplane A for aileron rolls from trimmed flight the agreement was good between the maximum sideslip angle and the variation of sideslip angle with time between the step-by-step solution and the solution of the linearized lateral equations including product-of-inertia terms for airplane B (figs. 10 and 11). These results also indicate that the pitching motion and resulting cross-couple inertia terms $(I_x-I_r)\theta\dot{\phi}$ and $(I_r-I_z)\theta\dot{\psi}$ for rolls from trimmed flight are not sufficient to influence the maximum sideslip angle.

For airplane B the rolling velocity $\dot{\phi}$ varied widely because of the dihedral effect resulting from the large sideslip angles. Maximum values of $pb/2V$ of 0.041 and 0.048 were obtained for loadings 1 and 2, respectively. The value of $\Delta C_l/C_{l_p}$, the steady-state value of $pb/2V$ for the rolling degree of freedom, was 0.053. Substitution of $\Delta C_l/C_{l_p}$ for $pb/2V$ in the simplified expression of reference 3 (eq. (1)) therefore seems to be more nearly accurate for this airplane than it was for airplane A and the agreement of the simplified expression with the more complete solutions may be considered better for this airplane than for airplane A. It is of interest to note, however, that the simplified expression overestimated the maximum sideslip angle for airplane B, whereas it had underestimated the values for airplane A.

For both loadings for airplane B, the solution of the linearized lateral equations, excluding product-of-inertia terms, leads to larger maximum sideslip angles than were obtained when products of inertia were included (figs. 10 and 11). This result occurs primarily because the rolling acceleration was negative for some time prior to the time

the maximum sideslip angle was reached and the moment $I_{xz}\dot{\phi}$ in the yawing-moment equation was such as to reduce the sideslip angle.

The results for airplane B showed little influence of loading on the maximum sideslip angle (figs. 5 and 6) for aileron rolls from trimmed flight. The differences in loadings 1 and 2 for airplane B were a change in the value of both I_x and I_z (table II). Since the small value of C_{n_β} for airplane B led to large values of sideslip angles, the dihedral effect $C_{l_\beta}\beta$ became a predominant moment in roll and the resultant rates of roll for both loadings for most of the motion were not appreciably different. The moment $C_{n_p}\dfrac{pb}{2V}$ was, therefore, similar for both loadings, this similarity contributing in part to the agreement in sideslip angles for the two loadings.

For both loadings on airplane B, an oscillation in angle of attack was started about the initial trim angle of attack, the oscillation tending to be divergent (figs. 5(b) and 6(b)). Maximum deviations of $3\frac{1}{2}°$ and $7\frac{1}{2}°$ from the trim angle of attack were obtained for loadings 1 and 2, respectively. For this airplane the cross-couple inertia moment in pitch $(I_z-I_x)\dot{\phi}\dot{\psi}$ changed sign during the motion in that the values of $\dot{\phi}$ and $\dot{\psi}$ changed sign; whereas for airplane A these values were of constant sign. This variation of sign of this moment may have augmented the oscillation in angle of attack. It appears that, if the motion were allowed to progress, larger variations in angle of attack and even negative angles of attack may be encountered. Variations of angle of attack of this type as encountered in rolling maneuvers may be problems for consideration in horizontal-tail designs.

Because accelerations along the Z-axis were not considered, the effect of $\partial C_L/\partial\alpha$ was neglected. The effect of $\partial C_{m_\alpha}/\partial\alpha$ was also neglected, since this derivative was omitted from the pitching equation. Inclusion of these factors would have caused a somewhat more heavily damped pitching oscillation and somewhat smaller variations in angle of attack than are presented. The effects of pitching caused by changes in angle of attack on the sideslip angle, through the cross-couple inertia moments, have, however, been shown to be relatively small; whereas the effect of an initial pitching velocity (which is not influenced by the omissions discussed) as in the 6g pull-up for airplane A does have some influence on the sideslip angles.

COMPARISON OF AIRPLANES A AND B

As has previously been noted, the second loading for airplane B is nearly the same as loading 1 for airplane A; therefore, the significant difference in the results in figures 2 and 6 (maximum values of β of $5\frac{1}{4}°$ and $24\frac{1}{2}°$, respectively) is caused by differences in the aerodynamic forces and moments acting. One primary difference for these two cases is the value of C_{n_β} (directional-stability derivative). For low

values of C_{n_β} (airplane B) large values of sideslip angle were obtained (about 25°); whereas for large values of C_{n_β} (airplane A) small values of maximum sideslip angle were obtained (about 5°). It appears, therefore, that C_{n_β} is a critical parameter for vertical-tail design.

As has previously been noted, changes in loading for airplane A had an appreciable effect on the maximum angle of sideslip; whereas changes in loading for airplane B had relatively little influence on the maximum sideslip angle. For airplane A, for which the angles of sideslip were relatively small (of the order of 5°) because of the large value of C_{n_β}, the change in loading caused primarily a change in the rate of roll and the yawing moments $C_{n_p} \frac{pb}{2V}$ were appreciably different. This moment contributed to the differences in sideslip angle. For airplane B the relatively small value of the directional-stability derivative C_{n_β} allowed the airplane to reach large sideslip angles, and the dihedral effect arising from these large sideslip angles caused the rates of roll to be small and similar for both loadings such that the contributions of $C_{n_p} \frac{pb}{2V}$ were similar, as were the resultant sideslip angles.

For airplanes of current design for high-speed high-altitude flight, the trends in aerodynamic characteristics, particularly increasing values of C_{n_β}, appear to be such as to cause smaller sideslip angles in rolling maneuvers than were encountered with the World War II type of airplane. The changes in aerodynamic characteristics appear, therefore, to cause a change in the order of magnitude of the maximum sideslip angles. It is important to note, however, that vertical-tail sizes as well as airspeeds have tended to increase for these current designs and hence the vertical-tail loads may be large in spite of the smaller sideslip angles. Changes in mass distribution appear to influence critically the maximum sideslip angle only for airplanes of current design where the sideslip angles may be relatively small.

CONCLUSIONS

The results of the investigation presented herein give the following indications with regard to sideslip angles and resultant vertical-tail loads in rolling maneuvers for current high-speed airplanes:

1. Existing simplified expressions for calculating maximum sideslip angles in rolling maneuvers will greatly underestimate the maximum sideslip angle for some conditions.

2. Solution of the three linearized lateral equations of motion, including product-of-inertia terms, will generally indicate with sufficient accuracy the sideslip angles expected in aileron rolls from trimmed flight.

3. In rolling pullouts where the pitching velocity is large, inclusion of the equation of pitching motion along with the lateral equations of motion and consideration of cross-couple inertia terms is necessary to obtain the maximum sideslip angles accurately.

4. Trends in aerodynamic characteristics, particularly increasing values of C_{n_β} (the rate of change of the yawing-moment coefficient due to sideslip), appear to be such as to cause smaller maximum sideslip angles than were encountered in the past although the vertical-tail loads may be large because of the higher airspeeds. For the case of large C_{n_β}, variations in mass distribution may critically affect the maximum sideslip angle.

5. Pitching oscillations started during the rolling motion will be influenced by cross-couple inertia moments and may cause large variations in angle of attack which affect the horizontal-tail loads.

Langley Aeronautical Laboratory,
    National Advisory Committee for Aeronautics,
      Langley Field, Va., *December 7, 1951.*

REFERENCES

1. Gilruth, Robert R.: Analysis of Vertical-Tail Loads in Rolling Pull-Out Maneuvers. NACA WR L–181, 1944. (Formerly NACA CB L4H14.)
2. Wolowicz, Chester H.: Prediction of Motions of an Airplane Resulting From Abrupt Movement of Lateral or Directional Controls. NACA WR L–125, 1945. (Formerly NACA ARR L5E02.)
3. White, Maurice D., Lomax, Harvard, and Turner, Howard L.: Sideslip Angles and Vertical-Tail Loads in Rolling Pull-Out Maneuvers. NACA TN 1122, 1947.
4. Jones, B. Melvill: Dynamics of the Aeroplane. The Asymmetric or Lateral Moments. Vol. V of Aerodynamic Theory, div. N, ch. III, secs. 10 and 21, W. F. Durand, ed., Julius Springer (Berlin), 1935, pp. 61, 71–72.
5. Johnson, Joseph L., and Sternfield, Leonard: A Theoretical Investigation of the Effect of Yawing Moment Due to Rolling on Lateral Oscillatory Stability. NACA TN 1723, 1948.
6. Michael, William H., Jr.: Analysis of the Effects of Wing Interference on the Tail Contributions to the Rolling Derivatives. NACA Rep. 1086, 1952. (Supersedes NACA TN 2332.)
7. Weick, Fred E., and Jones, Robert T.: The Effect of Lateral Controls in Producing Motion of an Airplane as Computed From Wind-Tunnel Data. NACA Rep. 570, 1936.
8. Phillips, William H.: Effect of Steady Rolling on Longitudinal and Directional Stability. NACA TN 1627, 1948.